

## Avalanche dynamics in a pile of rice

Vidar Frette\*, Kim Christensen,  
Anders Malthe-Sørenssen, Jens Feder,  
Torstein Jøssang & Paul Meakin

Department of Physics, University of Oslo, PO Box 1048, Blindern, N-0316 Oslo, Norway

**THE idea of self-organized criticality<sup>1</sup> (SOC) is commonly illustrated conceptually with avalanches in a pile of sand grains. The grains are dropped onto a pile one by one, and the pile ultimately reaches a stationary 'critical' state in which its slope fluctuates about a constant angle of repose, with each new grain being capable of inducing an avalanche on any of the relevant size scales. Some numerical models of sand-pile dynamics do show SOC<sup>1-8</sup>, but the behaviour of real sand piles remains ambiguous<sup>9-18</sup>. Here we describe experiments on a granular system—a pile of rice—in which the dynamics exhibit self-organized critical behaviour in one case (for grains with a large aspect ratio) but not in another (for less elongated grains). These results show that SOC is not as 'universal' and insensitive to the details of a system**

as was initially supposed<sup>1</sup>, but that instead its occurrence depends on the detailed mechanism of energy dissipation.

We have studied the dynamics of piles of rice for several system sizes (Fig. 1). Grains of rice were slowly fed into the gap between two vertical, parallel plates. Mass accumulated in the pile until it reached a quasi-stationary state. Under continued addition, avalanches redistributed mass along the surface layer of the heap and transported mass out of the system, thereby changing the profile. The anisotropy of the grains (see Table 1) gave rise to a variety of packing configurations<sup>7</sup> (Fig. 1). The anisotropy restricted the way the grains moved down the slope, enhanced the frictional contact and, to a large extent, suppressed inertia effects. The size of an avalanche was defined as the energy dissipated between two consecutive profiles (Fig. 2*a, b*). A temporal sequence of avalanche sizes for rice A is shown in Fig. 2*c*. There was a large variation in the avalanche sizes and an apparently chaotic structure in time. We concentrate here on the statistics of the avalanche sizes.

Based on experience with a wide range of complex systems, it is reasonable to expect that the probability density  $P(E, L)$ , where  $P(E, L)dE$  is the probability that an avalanche with energy dissipation between  $E$  and  $E + dE$  will occur in a system of size  $L$ , will have the form

$$P(E, L) = L^{-\beta} f(E/L^{\nu}) \quad (1)$$

where the scaling function  $f$  and the scaling exponents  $\beta$  and  $\nu$  are to be determined. From the normalization  $\int_0^{\infty} P(E, L)dE = 1$  it follows that  $\beta = \nu$ . Further, in the stationary state, the average

\* Present address: Department of Physics of Complex Systems, The Weizmann Institute of Science, Rehovot 76100, Israel.

TABLE 1 Types of rice used in experiments

	Rice A	Rice B	Rice C
Name	Geisha* <i>naturris</i>	Geisha* <i>grøtris</i>	Geisha* <i>middagsris</i>
Description	Unpolished (rough)	Polished (smooth)	Polished (smooth)
Length, $\delta$	$7.6 \pm 0.9$ mm	$4.8 \pm 0.4$ mm	$6.9 \pm 1.0$ mm
Width	$2.0 \pm 0.1$ mm	$2.4 \pm 0.2$ mm	$1.9 \pm 0.1$ mm
Aspect ratio	3.8	2	3.6
Average mass, $m$	0.02066 g	0.01840 g	0.01874 g
No. density	$37 \pm 1$ grains $\text{cm}^{-3}$	$43 \pm 1$ grains $\text{cm}^{-3}$	$44 \pm 1$ grains $\text{cm}^{-3}$
Energy unit, $\varepsilon$	$1.54 \mu\text{J}$	$0.867 \mu\text{J}$	$1.27 \mu\text{J}$
Angle of repose	$48.4^\circ \pm 1.2^\circ$	$46.6^\circ \pm 0.8^\circ$	$51.1^\circ \pm 2.0^\circ$

The large variation in length for rice A and C adds to the inhomogeneity of the system (Fig. 1). The average grain mass,  $m$ , was obtained by weighing 2,500 grains. The number density is the average number of grains per unit volume. The energy unit is  $\varepsilon = mg\delta$ , where  $g$  is the acceleration of gravity and  $\delta$  is the grain length. Throughout the Letter we express the energy dissipation in units of  $\varepsilon$ , that is, by the dimensionless quantity  $E = \mathcal{E}/\varepsilon$ , where  $\mathcal{E}$  is the energy dissipation of an avalanche. Similarly, we express the system size  $\mathcal{L}$  by the dimensionless number  $L = \mathcal{L}/\delta$ . The average pile height at the vertical wall was used to estimate the angle of repose. The standard deviation in this angle reflects the observed height fluctuations.

\* Geisha is a registered trademark from Stabburet a.s. (Trollåsen, Norway).

dissipated energy  $\langle E \rangle = \int_0^\infty EP(E, L)dE / \int_0^\infty P(E, L)dE \propto L^\nu$  is equal to the average added potential energy. Because the angle of repose varied only weakly with system size, the added potential energy was proportional to  $L$ . Thus  $\langle E \rangle \propto L$ , and  $\nu = 1$ .

Figure 3a shows the probability density  $P(E, L)$  for rice A with system sizes of  $L = 16, 33, 66$  and  $105$  (see Table 1). The behaviour can be described by a scaling function of the form  $f(x) = \text{const.}$  for  $x < 1$ , and  $f(x) \propto x^{-\alpha}$  for  $x > 1$ . Figure 3b shows a finite-size scaling plot of these results with  $\beta = \nu = 1$ . There is a reasonably good data collapse. The exponent  $\alpha$  was estimated from fits in the range  $6 \leq E/L \leq 300$ . We found size-dependent corrections to scaling for the exponent  $\alpha$  of the form  $\alpha = \alpha_\infty + l/L$ , with  $l \approx 8.6$ , where  $\alpha_\infty \approx 2.06$  is the power-law exponent in a system with  $L \rightarrow \infty$ . From data covering the range  $10 \leq E/L \leq 100$ , we found  $\alpha_\infty \approx 2.02$  and  $l \approx 10.4$ . We conclude that  $\alpha_\infty$  is slightly above 2 and  $l = 9.5 \pm 1$ . The avalanche

dynamics in the rice pile with the elongated rice A is consistent with a self-organized critical process.

Figure 4a shows the probability density  $P(E, L)$  for rice B with  $L = 26, 52$  and  $104$ . Using  $\nu = \beta = 1$ , we find that the probability densities are consistent with a stretched-exponential scaling function,  $f(x) \propto \exp(-(x/x^*)^\gamma)$  with  $\gamma \approx 0.43$  and  $x^* \approx 0.45$  (Fig. 4b). A characteristic avalanche size  $E^* = x^*L$  for the dynamics of rice B appears, which is inconsistent with the idea of SOC.

We conclude that SOC behaviour is not a universal characteristic of slowly driven granular media. A difference in the detailed relaxation mechanisms for rice A and the more isotropic rice B might explain the crossover from a critical to a non-critical behaviour. For the elongated rice A, the relaxation dynamics was dominated by (1) 'domains' of grains that moved slowly, coherently and intermittently, while keeping most of their 'solid-like' internal structure, and (2) many 'individual' grains that

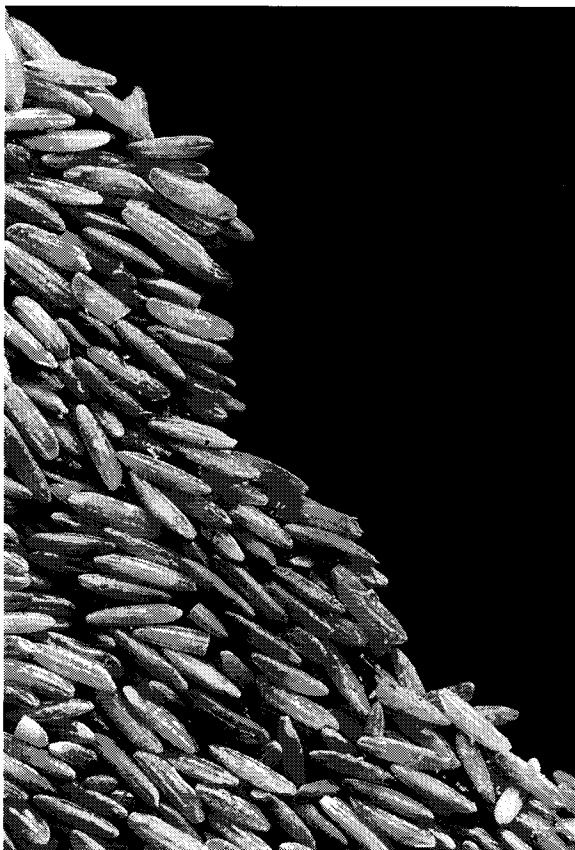


FIG. 1 A close-up photograph of a pile of rice A (see Table 1). Piles of rice were confined between two 5-mm-thick glass plates supported by  $100 \times 120$  cm polymethylmethacrylate plates (15 mm thick). Aluminium rods formed the vertical wall and the variable one-dimensional base of the pile (Fig. 2a, b). All the experiments were performed with a constant plate-separation to grain-length ratio of  $\sim 0.8$ . In an extensive series of experiments, we did not find any qualitative changes as the plate separation was varied. As shown, most of the grains were aligned along the flow direction, but there was a significant spread in the angular orientation of the grains, and a variety of packing configurations were obtained. As a result, the local slope varied considerably along the profile. These 'patterns' of steep and flat portions in the profile changed substantially in time. The dynamics of the rice piles was recorded with a photometric CCD (charge-coupled device) camera (CH250 from Photometrics, Tucson, Arizona) with a spatial resolution of  $2,000 \times 2,000$  pixels, and 12-bit grey-level resolution. For each system size, we chose lens and camera distance so that a  $2,000 \times 500$  pixels picture segment covered the active zone of the pile. Grains were injected at the vertical wall at a rate of  $20$  grains  $\text{min}^{-1}$ . Frames were taken at 15 s intervals and the profiles (typically  $\sim 2,800$  pixels) were identified. Each experiment lasted  $\sim 42$  h and consisted of 10,000 profiles. Our choice of feeding and sampling rates represent a compromise between the ideal of infinitely slow driving and the need to explore much of the large configuration space of the system.

flowed like a fluid along the profile. Occasionally, almost stagnant domains suddenly collapsed and released a flow, but frequently, the avalanches were initiated from above by flowing grains or from below through undermining as regions further down slid off. Series of such underminings constituted back-avalanches<sup>2</sup> that slowly and intermittently propagated upwards on the pile. Sometimes, single grains bounced through the system, but the frequency of these bouncing events decreased when  $L$  increased. This may have contributed to the decrease of the power-law exponent  $\alpha$  as the system size was increased.

Whereas grains of rice A slide along the surface, the more spherical rice B tended to roll. The dynamics of rice B consisted mainly of single grains that bounced rapidly down the slope or many 'individual' grains that flowed like a fluid along the profile. The grains often accumulated kinetic energy as they moved down the slope and were not easily halted. Typically, they propagated halfway through the system, independent of system size. Thus the rolling grains of rice B frequently tested the stability throughout the slope of the pile, and the fluctuations around the 'mean' profile were smaller than for the elongated

rice A. Furthermore, this 'inertia effect' led to a non-local process whereas in the numerical models displaying SOC and the rice pile with elongated grains, the dynamics was dominated by local mechanisms.

In an experiment with a third rice C (elongated like rice A, smooth like rice B; Table 1) we observed sliding mechanisms and profile shapes similar to rice A and the probability density was again a power law. This suggests that the statistics of the relaxation events is dominated by the shape rather than the surface properties of the grains. A large aspect ratio leads to a 'rough' profile and a sliding grain motion with a higher effective friction, which is crucial to getting 'critical dynamics'. It would be interesting to find a computer model in which a crossover from critical to non-critical behaviour is observed as a function of a relevant parameter, such as the ratio between the dissipation and the gain in kinetic energy as the grains move down the slope.

A reanalysis<sup>18</sup> of all the previous experiments<sup>9-17</sup> on granular systems shows that the flow over the rim of the pile ('drop numbers') has a stretched-exponential distribution inconsistent with the SOC hypothesis. By measuring the internal avalanches

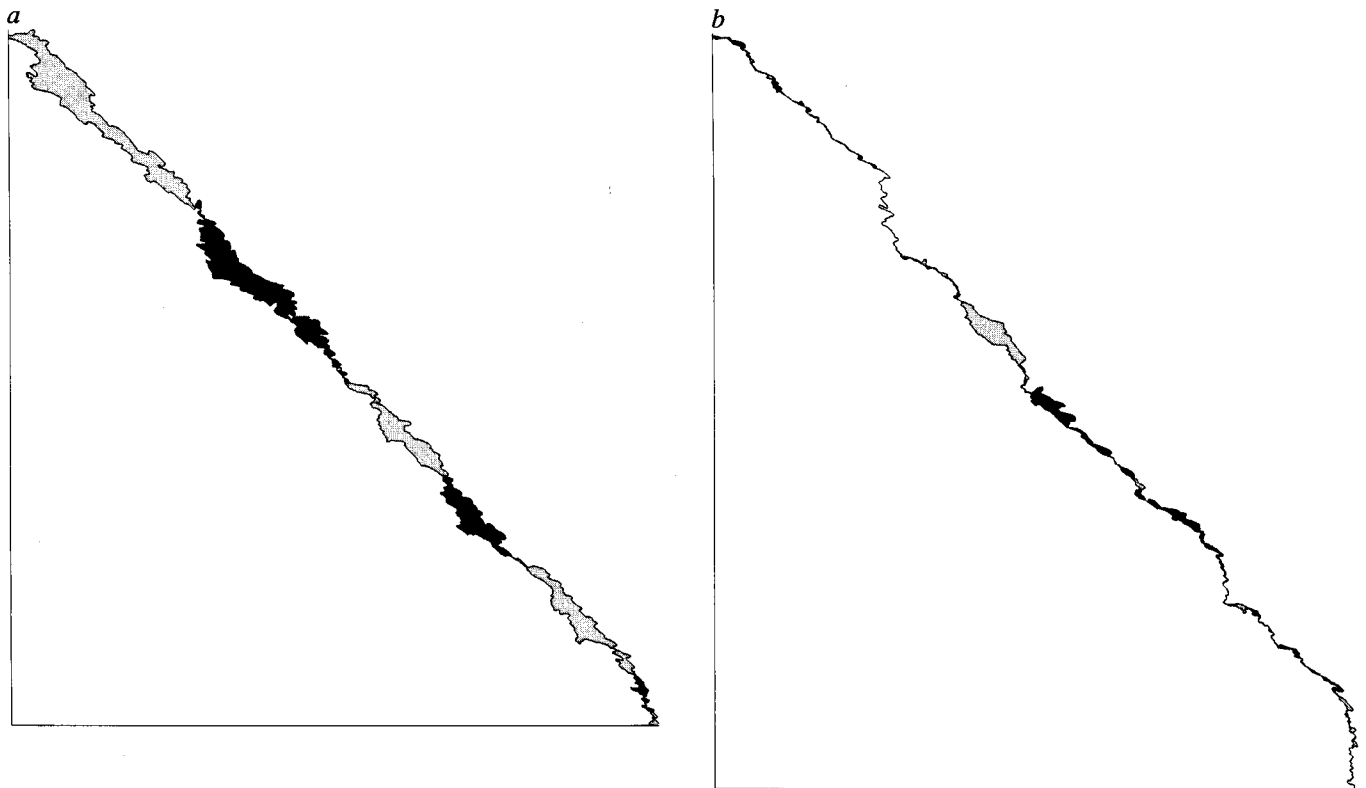
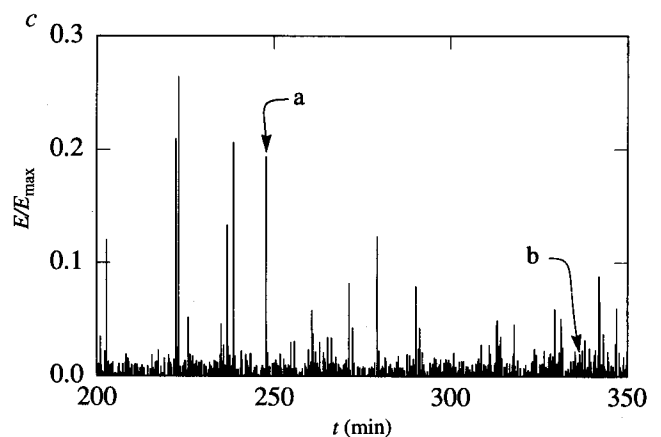


FIG. 2 *a, b*, Two avalanches of different sizes from an experiment with rice A at a plate separation of  $d/\delta = 0.79$  and system size of  $L = 33$  expressed in terms of the grain length  $\delta$  (see Table 1) (the baseline length in *a* and *b* was 25 cm = 1,548 pixels). In each case, two successive profiles have been plotted together. The areas enclosed by the two profiles represent the reorganization of mass in the pile. Loss (gain) of mass is indicated by grey (black) areas. Whenever grains have moved down the slope, potential energy has been lost and we measured the redistribution of mass in terms of dissipated potential energy. The sizes of these avalanches are 2,868 (*a*) and 294 (*b*). The energy dissipation is expressed in terms of  $\epsilon = mg\delta = 1.54 \mu\text{J}$  (see Table 1). Most of the grains slid some distance inside the pile, and only a smaller fraction reached the rim and left the system ('drop event'). The internal reorganizations (avalanches) reflect the response to the driving in a more direct way than the drop events. *c*, Temporal sequence of avalanche sizes for the experiment specified above. The size of each avalanche, rescaled by the maximal avalanche  $E_{\text{max}}$  for the entire experiment, is displayed as a vertical line. The sequence shown is a 2.5-h segment consisting of 600 avalanches. The arrows indicate the events shown in *a* and *b*.



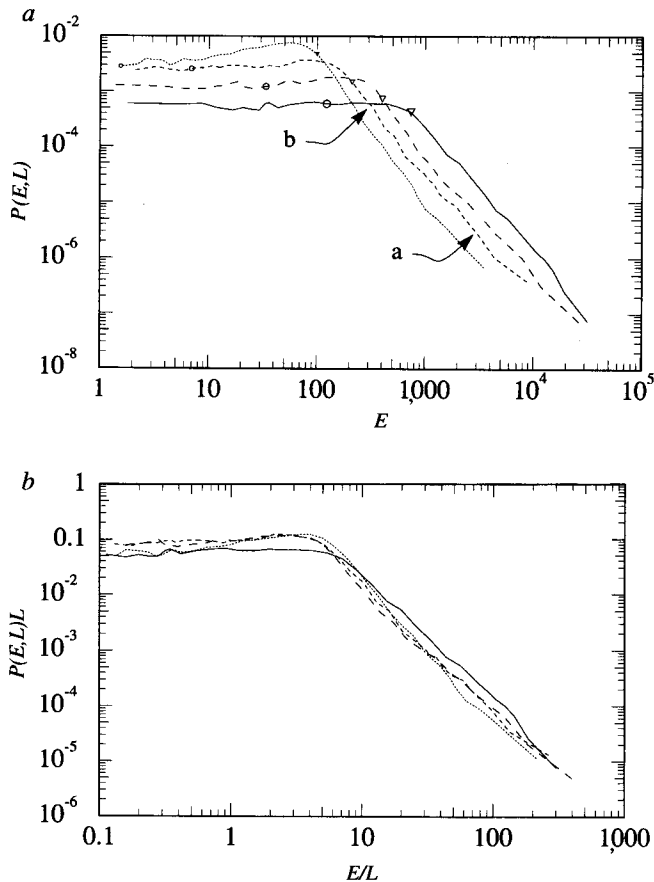


FIG. 3 a, Log-log plot of the probability density  $P(E, L)$  as a function of energy dissipation  $E$  for rice A, a plate separation of  $d/\delta = 0.79$ , and system sizes  $L = 16, 33, 66$  and  $105$ , marked with lines of increasing dash length. The energy dissipation is expressed in terms of  $\varepsilon = 1.54 \mu\text{J}$  and the system size in terms of the grain length  $\delta$  (see Table 1). The  $L = 16$  experiment was performed twice with very similar results for the probability density. The probability densities are constant for 'small' values of  $E$  and have a power-law form  $P(E, L) \propto E^{-\alpha}$ , extending over  $\sim 1\frac{1}{2}$  decades, for 'large'  $E$ , thus there is no characteristic avalanche size. The arrows show the avalanche sizes corresponding to the reorganization events in Fig. 2a, b. The average added energy between two profiles is indicated by triangles. This is taken into account when calculating the avalanche size. The noise level was determined by analysing a series of pictures (typically 5,000) of static profiles (no grain injection). The resulting probability densities have approximate exponential form with average 'avalanche' sizes indicated by circles. We were not able to get reliable results with our equipment beyond  $L = 105$  owing to limited resolution. In an  $L = 125$  experiment (not shown), the finer details such as the gaps between single grains at the surface of the pile were lost and the noise extended into the power-law range. However, the qualitative behaviour of the rice piles did not change as the system size was increased beyond  $L = 105$ . We measured the drop number for system sizes up to  $L = 263$  and found no indication of a crossover to the oscillatory behaviour observed in previous experiments on sandpiles<sup>9,10</sup>. b, A finite-size scaling plot of the data in a using equation (1) with  $\beta = \nu = 1$ . The scaling function has the form  $f(x) = \text{const.}$  for  $x < 1$  and  $f(x) \propto x^{-\alpha}$  for  $x > 1$ , with  $\alpha \approx 2.04$ . There are no obvious cutoffs in the scaling function, and the power-law behaviour extends up to the largest avalanche sizes measured in each case. In the scaling argument, a cutoff is unnecessary when the power-law exponent  $\alpha > 2$ .

for systems of different sizes, we have found that the theory of self-organized criticality applies to some slowly driven granular systems but is not a universal phenomenon. □

Received 12 January; accepted 13 November 1995.

1. Bak, P., Tang, C. & Wiesenfeld, K. *Phys. Rev. Lett.* **59**, 381–384 (1987); *Phys. Rev.* **A38**, 364–374 (1988).

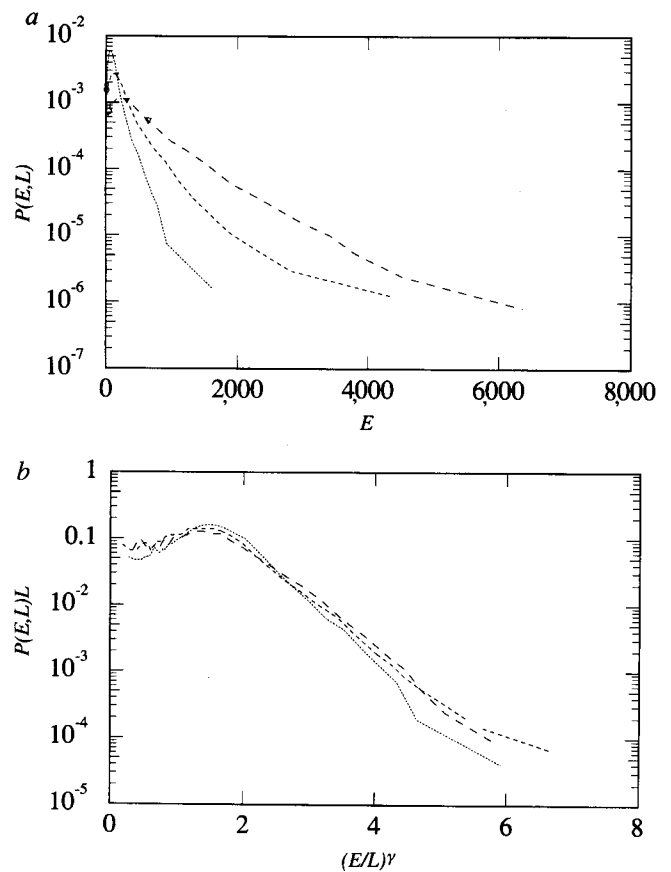


FIG. 4 a, Semi-log plot of the probability density  $P(E, L)$  as a function of energy dissipation  $E$  for rice B with a plate separation of  $d/\delta = 0.83$ , and system sizes  $L = 26, 52$  and  $104$ , indicated by increasing dash length for the curves. The energy was measured in terms of  $\varepsilon = 0.867 \mu\text{J}$  and the system size in terms of the grain length  $\delta$  (see Table 1). The average added energy between two profiles is indicated by triangles. This is taken into account when calculating the energy dissipation. The noise levels, determined in the manner explained in Fig. 3 legend, are indicated by circles. b, Scaling plot of the data in a with  $\beta = \nu = 1$ . The form of the scaling function in equation (1) is consistent with a stretched exponential,  $f(x) \propto \exp(-(x/x^*)^\gamma)$  with  $\gamma \approx 0.43 \pm 0.03$  and  $x^* \approx 0.45 \pm 0.09$ .

2. Kadanoff, L. P., Nagel, S. R., Wu, L. & Zhou, S.-m. *Phys. Rev.* **A39**, 6524–6537 (1989).  
 3. Carlson, J. M. & Langer, J. S. *Phys. Rev. Lett.* **62**, 2632–2635 (1989).  
 4. Feder, H. J. S. & Feder, J. *Phys. Rev. Lett.* **66**, 2669–2672 (1991); *Phys. Rev. Lett.* **67**, 283(E) (1991).  
 5. Olami, Z., Feder, H. J. S. & Christensen, K. *Phys. Rev. Lett.* **68**, 1244–1247 (1992).  
 6. Drossel, B. & Schwabl, F. *Phys. Rev. Lett.* **69**, 1629–1632 (1992).  
 7. Frette, V. *Phys. Rev. Lett.* **70**, 2762–2765 (1993).  
 8. Bak, P. & Sneppen, K. *Phys. Rev. Lett.* **71**, 4083–4086 (1993).  
 9. Jaeger, H. M., Liu, C.-h. & Nagel, S. R. *Phys. Rev. Lett.* **62**, 40–43 (1989).  
 10. Held, G. A. et al. *Phys. Rev. Lett.* **65**, 1120–1123 (1990).  
 11. Evesque, P. *Phys. Rev.* **A43**, 2720–2740 (1991).  
 12. Evesque, P., Fargeix, D., Habib, P., Luong, M. P. & Porion, P. *Phys. Rev.* **E47**, 2326–2332 (1993).  
 13. Bretz, M., Cunningham, J. B., Kurczynski, P. L. & Nori, F. *Phys. Rev. Lett.* **69**, 2431–2434 (1992).  
 14. Morales-Gamboa, E., Lomnitz-Adler, J., Romero-Rochin, V., Chicharro-Serra, R. & Peralta-Fabi, R. *Phys. Rev.* **E47**, R2229–R2232 (1993).  
 15. Grumbacher, S. K., McEwen, K. M., Halverson, D. A., Jacobs, D. T. & Lindner, J. *Am. J. Phys.* **61**, 329–335 (1993).  
 16. Rosendahl, J., Vekić, M. & Kelley, J. *Phys. Rev.* **E47**, 1401–1404 (1993).  
 17. Rosendahl, J., Vekić, M. & Rutledge, J. E. *Phys. Rev. Lett.* **73**, 537–540 (1994).  
 18. Feder, J. *Fractals* **3** 431–433 (1995).

ACKNOWLEDGEMENTS. We thank N. Aeinehchi, T. Engøy, S. Gundersen, U. Oxaal, R. J. Wallace and T. Waimann for their help at various stages of this project, and we also thank S. R. Nagel for discussions. This work was supported by VISTA, a research corporation between the Norwegian Academy of Science and Letters and Den norske stats oljeselskap a.s. (STATOIL), by NFR, the Research Council of Norway, and by Norsk Hydro a.s. K. C. was supported by The Danish Natural Science Research Council.